The EMBO Journal Vol.18 No.13 pp.3800–3807, 1999

Induced fit in initial selection and proofreading of aminoacyl-tRNA on the ribosome

Tillmann Pape, Wolfgang Wintermeyer and Marina Rodnina[1]

Institute of Molecular Biology, University of Witten/Herdecke, D-58448 Witten, Germany

[1]Corresponding author
e-mail: rodnina@uni-wh.de

The fidelity of aminoacyl-tRNA (aa-tRNA) selection by the bacterial ribosome is determined by initial selection before and proofreading after GTP hydrolysis by elongation factor Tu. Here we report the rate constants of A-site binding of a near-cognate aa-tRNA. The comparison with the data for cognate aa-tRNA reveals an additional, important contribution to aa-tRNA discrimination of conformational coupling by induced fit. It is found that two rearrangement steps that limit the chemical reactions of A-site binding, i.e. GTPase activation (preceding GTP hydrolysis) and A-site accommodation (preceding peptide bond formation), are substantially faster for cognate than for near-cognate aa-tRNA. This suggests an induced-fit mechanism of aa-tRNA discrimination on the ribosome that operates in both initial selection and proofreading. It is proposed that the cognate codon–anticodon interaction, more efficiently than the near-cognate one, induces a particular conformation of the decoding center of 16S rRNA, which in turn promotes GTPase activation and A-site accommodation of aa-tRNA, thereby accelerating the chemical steps. As kinetically favored incorporation of the correct substrate has also been suggested for DNA and RNA polymerases, the present findings indicate that induced fit may contribute to the fidelity of template-programed systems in general.

Keywords: aminoacyl-tRNA/fidelity/induced fit/proofreading/ribosome

Introduction

To accomplish the discrimination of correct and incorrect substrates, most enzymes possess specific binding sites that are tailored to the structure of the correct substrate or its transition state. While this is an adequate strategy for enzymes which have to recognize one particular substrate, it does not lend itself to enzymes that use several similar substrates to synthesize a polymer on a template. Examples are DNA and RNA polymerases as well as ribosomes, which recognize their substrates, nucleoside triphosphates or aminoacyl-tRNAs (aa-tRNAs), respectively, on the basis of complementary base pairing. These enzymes work with high fidelities, although model studies in aqueous solution show that the free energy difference of forming a correct base pair compared with an incorrect one is in the order of 10 kJ/mol, providing a maximum discrimination by ~100-fold in a single selection step. Thus, proofreading mechanisms of various kinds have been proposed which have in common the fact that the discriminatory interaction is used more than once, the selection steps being separated by irreversible energy-consuming steps. General selection schemes including proofreading have been suggested by Hopfield (1974) and Ninio (1975). By introducing successive selection steps, an ever increasing selectivity can be achieved, albeit at increasing energetic cost (Ehrenberg and Blomberg, 1980).

The mechanism of aa-tRNA selection on the ribosome is not sufficiently understood. On the basis of limited kinetic information, a two-step mechanism comprising initial selection before and proofreading after GTP hydrolysis has been put forward (Thompson, 1988, and references therein). Based on measured rates of GTP hydrolysis and peptide bond formation, Thompson and colleagues have proposed that the intrinsic rate of GTP hydrolysis by elongation factor Tu (EF-Tu) is independent of the tRNA, thereby providing an internal kinetic standard for translational accuracy. According to that model, cognate and near-cognate ternary complexes, unlike non-cognate ones, undergo GTP hydrolysis due to the long lifetime of their complex with the ribosome, and therefore have to be discriminated by subsequent proofreading. However, the distinction of cognate/near-cognate and non-cognate ternary complexes by the time they remain bound to the ribosome proved invalid (Rodnina *et al*., 1996). Furthermore, the conclusion that ternary complexes or aa-tRNAs are discriminated solely on the basis of different rejection rates in either initial selection or proofreading appears premature, since at the time, not all steps of A-site binding contributing to selection had been resolved, and some rate constants had been not measured with precision (Thompson, 1988).

The multi-step process of aa-tRNA binding to the A site of the ribosome is depicted in Figure 1. In the first step, a ternary complex of aa-tRNA with EF-Tu and GTP forms a labile complex with the ribosome (initial binding) (Rodnina *et al*., 1996). Subsequent codon recognition triggers GTP hydrolysis (Rodnina *et al*., 1995) which results in a large-scale conformational change of EF-Tu to the GDP-bound form (Dell *et al*., 1990; Abel *et al*., 1996; Polekhina *et al*., 1996). As a consequence, aa-tRNA is released from EF-Tu and enters the A site on the 50S ribosomal subunit (accommodation) to take part in peptide bond formation. Alternatively, aa-tRNA may be rejected from the ribosome at this stage (proofreading).

Here we present the results of a kinetic analysis of binding to poly(U)-programed ribosomes of a near-cognate aa-tRNA, Leu-tRNA$_2^{Leu}$ (anticodon GAG). Kinetic data were obtained by both fluorescence stopped-flow and

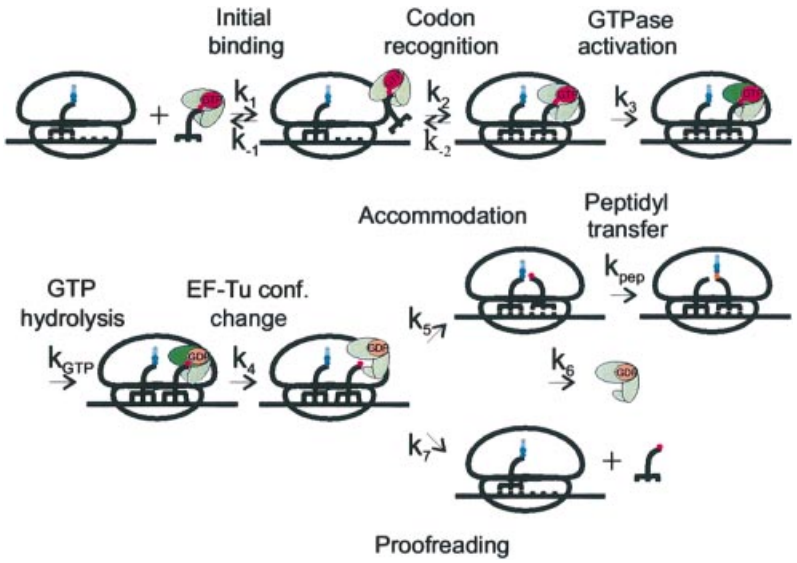

Fig. 1. Mechanism of EF-Tu-dependent binding of aa-tRNA to the ribosomal A-site. EF-Tu (light green) is depicted in three conformations: the GTP-bound form, the transient GTPase-activated form on the ribosome (G domain dark green) and the GDP-bound form that dissociates from the ribosome. Single arrows for steps 3–7 indicate insignificant backward rates; they do not imply strict irreversibility. See text for details.

quench-flow measurements. Elemental rate constants were obtained by global analysis of the time courses of reactions measured at various ribosome concentrations using numerical integration. By comparison with the respective rate constants determined previously for cognate aa-tRNA (Pape *et al*., 1998), we find that rearrangements of the aa-tRNA–ribosome complex (GTPase activation and A-site accommodation) that limit the rates of the chemical steps (GTP hydrolysis and peptide bond formation) are accelerated substantially in the cognate situation. This indicates an induced-fit mechanism of discrimination by conformational coupling which provides an important contribution to both initial selection and proofreading on the ribosome and, together with different rejection rates due to different stabilities of the codon–anticodon complexes, determines the overall fidelity of decoding.

Results

Rate constants of A-site binding

Kinetics of ribosome complex formation and of subsequent conformational transitions of aa-tRNA and EF-Tu were monitored by stopped flow using a proflavin-labeled fluorescent derivative of Leu-tRNA$_2^{Leu}$ (anticodon GAG) (Rodnina *et al*., 1996) or a fluorescent GTP derivative (mant-dGTP; Rodnina *et al*., 1995); rates of GTP hydrolysis and peptide bond formation were measured by quench flow (Pape *et al*., 1998). Kinetic experiments were performed at different ribosome concentrations (pseudo first-order conditions).

When poly(U)-programed ribosomes carrying AcPhe-tRNA^{Phe} in the P site are mixed with near-cognate ternary complex containing fluorescent Leu-tRNA$_2^{Leu}$, a biphasic fluorescence change is observed: a rapid increase is followed by a slower decrease (Figure 2A). The fluorescence increases by ~6% during initial binding of Leu ternary complex (Rodnina *et al*., 1996) and increases further upon codon recognition. Then the signal decreases, and the final fluorescence level is close to that of free tRNA. Since only a small fraction of Leu-tRNA$_2^{Leu}$ accommodates in the A site and forms dipeptide (see below; Figure 2D), the slow fluorescence decrease is attributed to the dissociation from the ribosome, in keeping with the similarity of final and initial signals.

Upon interaction of mant-dGTP-containing Leu ternary complex with the ribosome, a biphasic fluorescence change was observed (Figure 2B). The two phases represent the conformational transition of EF-Tu to the GTPase state (fluorescence increase) and the dissociation of EF-Tu·GDP from the ribosome (fluorescence decrease) (Rodnina *et al*., 1995). It has been shown previously that the fluorescence of mant-GTP (which allows GTPase activation to be monitored) is the same in the GTP and GDP forms of EF-Tu, i.e. there is no change due to GTP hydrolysis. The increase of mant fluorescence occurs on the ribosome, provided codon recognition takes place, but is not due to direct shielding of the dye by the ribosome; the activated (high fluorescence) state can be frozen immediately after GTP hydrolysis on the ribosome by kirromycin (Rodnina *et al*., 1995). Furthermore, for the EF-Tu mutant, G222D, the rate of GTPase activation (monitored by mant fluorescence) was found to be significantly faster than that of GTP hydrolysis (quench flow) (Vorstenbosch *et al*., 1996). Hence GTPase activation, as monitored by mant fluorescence, and GTP hydrolysis are physically distinct steps, although as shown below, the latter step is kinetically limited by the former.

Time courses of GTP hydrolysis and peptide bond formation observed with Leu ternary complex are shown in Figure 2C and D; the respective time courses observed with cognate Phe-tRNA^{Phe} (Pape *et al*., 1998) are shown for comparison. While the extent of GTP hydrolysis was close to 100% in both cases (Figure 2C), the rate of GTP hydrolysis was significantly lower for the Leu ternary complex. The efficiencies of dipeptide formation were drastically different for Phe and Leu; while Phe was virtually completely incorporated into AcPhePhe dipeptides, the efficiency of AcPheLeu dipeptide

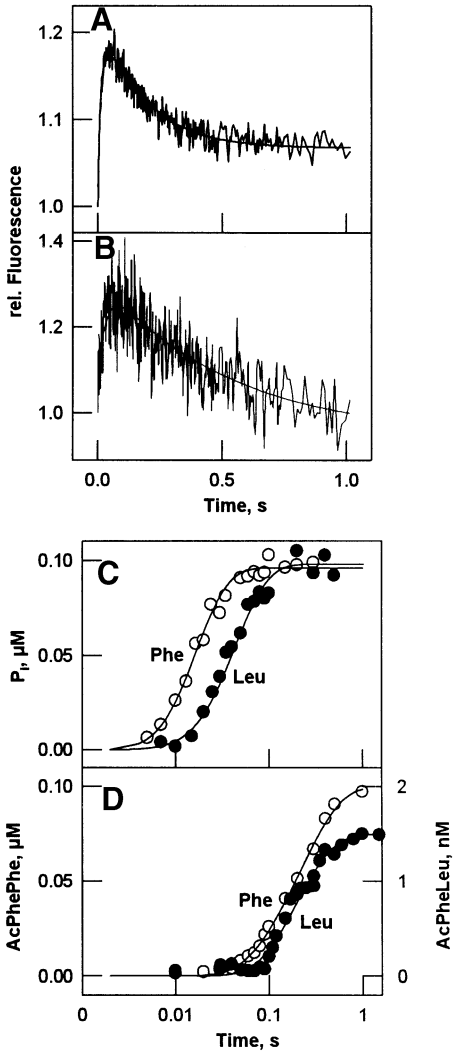

Fig. 2. Time courses of A-site interactions of Leu ternary complex. (**A**) Conformational changes of aa-tRNA monitored by the fluorescence of Leu-tRNA$_2^{Leu}$(Prf16/17/20). Parameters of two-exponential fits: k_{app1} = 65/s, A_1 = 22%, k_{app2} = 6/s, A_2 = –16%. (**B**) Conformational changes of EF-Tu monitored by mant-dGTP fluorescence. Parameters of two-exponential fits: k_{app1} = 44/s, A_1 = 37%, k_{app2} = 2/s, A_2 = –35%. (**C**) GTP hydrolysis in EF-Tu·[γ-^{32}P]GTP·Leu-tRNA$_2^{Leu}$ (●; k_{app} = 37/s) and EF-Tu·[γ-^{32}P]GTP·Phe-tRNA^{Phe} (○; k_{app} = 55/s). (**D**) Dipeptide formation with [^{3}H]Leu-tRNA$_2^{Leu}$ (●) or [^{3}H]Phe-tRNA^{Phe} (○). Concentrations after mixing were 0.1 μM ternary complex and 2 μM ribosomes. Note the different ordinates for Phe and Leu in (D). Smooth lines show time curves calculated from elemental rate constants (Table I).

formation was low (1.5%; Figure 2D), indicating a high rate of rejection and a low rate of accommodation for Leu, and the opposite for Phe. The similarity of the apparent rate constants of dipeptide formation for Phe and Leu (Figure 2D) is incidental; it is due to the fact that the sum of the rate constants of rejection and accommodation, which defines k_{app}, is approximately the same, although the individual rate constants are quite different (cf. Table I). The lag phases seen in Figure 2D are discussed below.

For an initial qualitative inspection, concentration dependencies of apparent rate constants were derived (Figure 3; filled symbols); for comparison, the respective data for the cognate Phe ternary complex (Pape *et al*., 1998) are included (open symbols). k_{app} values of codon recognition (fluorescence increase; Figure 2A) are about the same for Leu and Phe (Figure 3A). k_{app} values of the following two steps, GTPase activation (fluorescence increase, Figure 2B) and GTP hydrolysis (Figure 2C), are similar for Leu, and significantly lower than the corresponding values for Phe (Figure 3B). Since GTPase activation and GTP hydrolysis are physically distinct steps (Rodnina *et al*., 1995; Vorstenbosch *et al*., 1996), their similar rates suggest that GTPase activation is rate-limiting for GTP hydrolysis. Therefore, for global fitting, the two steps were grouped, and the rate determined from both the mant-dGTP fluorescence increase and GTP hydrolysis is referred to as the GTPase rate. The fluorescence decrease (Figure 2A) reflects the dissociation of the fluorescent Leu-tRNA$_2^{Leu}$ from the ribosome; k_{app} = 6/s, independent of the ribosome concentration (not shown). The apparent rate constant of EF-Tu·GDP dissociation from the ribosome (fluorescence decrease; Figure 2B) is ~2/s, independent of the ribosome concentration (not shown). Additional information is derived from the lag phase of dipeptide formation (Figure 2D). It is significantly longer than the time delay due to the reactions up to GTP hydrolysis (Figure 2C), indicating an additional step between GTP hydrolysis and accommodation. It is assigned to the expected large conformational change of EF-Tu from the GTP to the GDP form (Abel *et al*., 1996; Polekhina *et al*., 1996), which precedes the release of aa-tRNA from EF-Tu (Dell *et al*., 1990) and the accommodation in the A-site.

Global fitting does not yield a unique solution for the reaction mechanism of Figure 1, unless there is additional information; here it was sufficient to use directly measured values of two rate constants, k_{-1} and k_{-2}, and the relative fluorescence quantum yield of the initial binding complex P_c (see Materials and methods). k_{-1}, the dissociation rate constant of the initial binding complex, and P_c have been determined previously (Rodnina *et al*., 1996). k_{-2}, the dissociation rate constant of the codon recognition complex, was measured by chase experiments as follows. In the presence of non-hydrolyzable GTP analogs, such as GDPNP, A-site binding is blocked after the codon recognition step (Kaziro, 1978), while the rate of codon recognition is unaffected (Rodnina *et al*., 1994). Thus, to determine k_{-2}, the pre-formed complex of EF-Tu·GDPNP·Leu-tRNA$_2^{Leu}$(Prf16/17/20) with poly(U)-programed ribosomes was mixed rapidly with a 10-fold excess of unlabeled EF-Tu·GDPNP·Phe-tRNA^{Phe} in the stopped-flow apparatus and the dissociation of the complex followed by the fluorescence decrease (Figure 4). Single-exponential fitting yielded k_{app} = 17/s, the value of k_{-2}.

For the calculation of the remaining elemental rate constants of the mechanism depicted in Figure 1, combined data sets containing time courses obtained with all observables (proflavin fluorescence, mant-dGTP fluorescence, GTP hydrolysis and dipeptide formation) at four different ribosome concentrations were fitted globally by numerical integration. In addition to using fixed values of k_{-1} and k_{-2}, the tRNA fluorescence in the initial binding complex relative to the unbound ternary complex was set to 1.06 (Rodnina *et al*., 1996). The rate constants obtained for near-cognate Leu-tRNA$_2^{Leu}$ are presented in Table I along with the previously reported data for cognate Phe-tRNA^{Phe} (Pape *et al*., 1998).

Table I. Elemental rate constants of near-cognate (Leu) and cognate (Phe)[a] aa-tRNA binding to the A site according to the model presented in Figure 1

Step	Rate constant (per s)		
		Near-cognate	Cognate[a]
Initial binding	k_1	110 ± 10[b]	110 ± 20[b]
	k_{-1}	25 ± 5[c]	25 ± 5[c]
Codon recognition	k_2	100 ± 20	100 ± 15
	k_{-2}	17 ± 8[d]	0.2 ± 0.1
GTPase activation and GTP hydrolysis[e]	k_3	50 ± 20	500 ± 100
GTP–GDP conformation change of EF-Tu	k_4	50 ± 20	60 ± 20
aa-tRNA accommodation and peptide bond formation[e]	k_5	0.1 ± 0.03	7 ± 2
Dissociation of EF-Tu	k_6	2 ± 1	3 ± 1
aa-tRNA rejection	k_7	6 ± 1	<0.3

[a]From Pape *et al*. (1998).
[b]per μM/s.
[c]Determined independently (Rodnina *et al*., 1996).
[d]Determined independently (Figure 4).
[e]Grouped for analysis, because the former reaction is rate limiting.

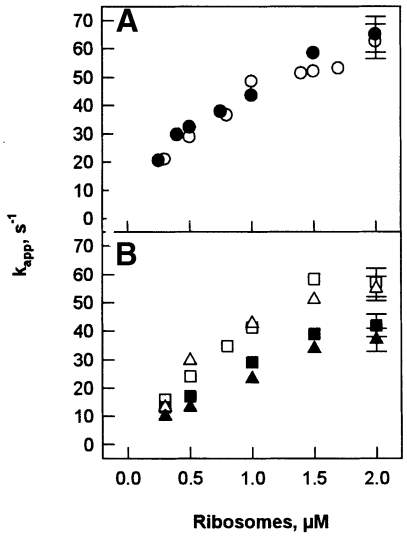

Fig. 3. Concentration dependence of k_{app} of (**A**) codon recognition (●), and (**B**) GTPase activation (■) and GTP hydrolysis (▲) for Leu ternary complex. Respective open symbols indicate the values observed previously for Phe (Pape *et al*., 1998) where the three steps have the same apparent rate constants. Standard deviations did not exceed 10% of the measured value.

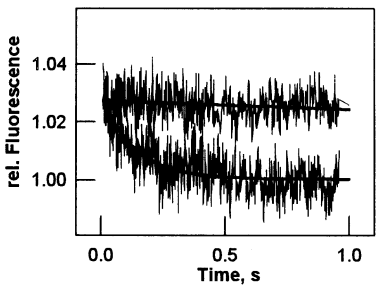

Fig. 4. Determination of the dissociation rate constant of the near-cognate codon recognition complex; exponential fitting yields k_{-2} = 17/s. Upper trace, control.

As expected, the rate constants of initial binding are the same for Leu and Phe (k_1 = 110/μM/s), similar to the value determined in the poly(A) system (60/μM/s) (Rodnina *et al*., 1996). The dissociation rate constants of initial binding complex are identical for Leu and Phe (k_{-1} = 25/s) (Rodnina *et al*., 1996). The forward rate constants of codon recognition are the same for Leu and Phe (k_2 = 100/s), whereas the corresponding dissociation rate constants, k_{-2}, differ ~100-fold. Unexpectedly, the GTPase rate constants, k_3, are also very different (50 and 500/s). The rate constant of the conformational change of EF-Tu from the GTP to the GDP form (k_4), ~60/s, is the same. For the accommodation in the A site, rate constants (k_5) of 0.1 and 7/s are obtained for Leu and Phe, respectively. In both cases, the rate-limiting accommodation step is followed instantaneously by peptide bond formation. The accommodation step is highly efficient for cognate Phe-tRNA^{Phe}, since ~95% of added ternary complex reacts to form dipeptide. Assuming a 5% drop-off of Phe-tRNA^{Phe} at this stage, the maximum rate constant of dissociation (k_7) would be 0.3/s; the true value is probably much smaller, since the missing 5% of dipeptides presumably are due mainly to incomplete activity of the ribosomes. In contrast, the comparably large value of the rate constant of Leu-tRNA$_2^{Leu}$ rejection, k_7 = 6/s, is well defined. The partitioning of Leu-tRNA$_2^{Leu}$ between accommodation (k_5 = 0.1/s) and rejection (k_7 = 6/s) explains why the efficiency of Leu misincorporation is low (1.5%; Figure 2D), even in the absence of competing cognate ternary complex. The rate constant of EF-Tu·GDP dissociation from the ribosome (k_6) is similar in both cases.

From the elemental rate constants of Table I, time courses for various observables were calculated for different concentrations of ribosomes; the results are shown in Figure 2 along with the experimental data.

Fidelity of aa-tRNA selection

In vivo, different ternary complexes compete for the A site. This situation was modeled using the elemental rate constants (Table I) to calculate the frequency of Leu misincorporation as well as the contribution of initial

Table II. Fidelity of dipeptide formation and translation

Mg^{2+}	Error frequency		
	Dipeptide[a]		Translation[b]
	Measured	Calculated	
10 mM	$(1.3 \pm 0.5) \times 10^{-2}$	1.4×10^{-2}	2×10^{-2}
5 mM	$(9 \pm 8) \times 10^{-4}$		3×10^{-3}

[a]Measured values were obtained from the normalized selectivity of dipeptide formation (Equation 1, Materials and methods; Ehrenberg *et al*., 1990), where v_c and v_i are the concentrations of AcPhePhe and AcPheLeu dipeptides formed, respectively, as determined experimentally. Experiments were performed with 0.1 μM ribosomes and equal (0.2–0.3 μM) concentrations of Phe and Leu ternary complexes. After incubation for 30 s at 20°C, reactions were stopped and analyzed as described (Vorstenbosch *et al*., 1996).
[b]Leu incorporation during poly(U) translation was measured at 20°C and evaluated as described (Ehrenberg *et al*., 1990), except that equal concentrations of purified Phe and Leu ternary complexes were used.

selection versus proofreading for a situation where cognate and near-cognate ternary complexes are present in equal concentrations, using a formalism described previously (Fersht, 1985). The efficiency of initial selection (f) is determined by the rate constants of initial binding, codon recognition and GTP hydrolysis (Figure 1) and is defined as $f = (k_{cat}/K_M)_{correct}/(k_{cat}/K_M)_{incorrect}$ of the GTPase. Since the values of k_2, k_{-2} and k_3 are similar, the expressions for k_{cat}/K_M were derived using the Briggs–Haldane formalism. With the equations derived for the mechanism of Figure 1 (see Materials and methods) and the pertinent rate constants for Phe and Leu (Table I), k_{cat}/K_M values for Phe and Leu of 88 and 82/μM/s, respectively, were obtained, indicating that there is practically no initial selection ($f = 1.07$) in the conditions under which the rate constants have been determined. Hence, the low misincorporation of Leu observed in these conditions has to be due to rejection in the proofreading step. The probability of incorporation of near-cognate Leu is $F_i = 0.015$ (F_c is close to 1 for cognate Phe). Accordingly, an overall selectivity of $S = f{\cdot}F_c/F_i = 72$ is achieved in the presence of competing ternary complexes, or an error frequency of $P_e = 1/(1 + S) = 1.4\times10^{-2}$.

The calculated value of the error frequency was verified experimentally by determining the fidelity of dipeptide formation and translation in the presence of about equal concentrations of cognate and near-cognate ternary complexes. The experimental value of the error frequency is

$$P_e \approx \frac{\text{AcPheLeu}}{\text{AcPhePhe}} \cdot \frac{[\text{Phe}]}{[\text{Leu}]} = 1.3\times10^{-2},$$

in good agreement with the calculated value and the overall translation error frequency observed experimentally (Table II). This provides strong support for the kinetic model and the rate constants of Table I. The similarity of error frequencies of dipeptide formation and overall translation suggests that the fidelity of translation is determined only by the selectivity of A-site binding, and that there are no additional selection steps.

The experimental conditions of the kinetic experiments (10 mM Mg^{2+}) were chosen to achieve measurable misincorporation of Leu, and it is therefore not surprising that the selectivity is not very high. It is known that a decrease in the Mg^{2+} concentration substantially increases the fidelity of aa-tRNA selection. Therefore, to determine the contribution of initial selection and proofreading under conditions of higher fidelity, we performed misincorporation experiments at 5 mM Mg^{2+}. In the absence of competing cognate ternary complex (i.e. no initial selection), the concentration of Leu-containing dipeptide formed is reduced 2-fold at 5 mM Mg^{2+} compared with at 10 mM (not shown), indicating that the efficiency of proofreading is increased to about $F_c/F_i = 120$ (compared with $F_c/F_i = 67$ at 10 mM Mg^{2+}). In the presence of equal concentrations of cognate and near-cognate ternary complexes, when there is initial selection due to competition, an overall error frequency of 9×10^{-4} was obtained, close to the value of 3×10^{-3} measured in translation (Table II). This suggests that, at the lower Mg^{2+} concentration, initial selection contributes a factor of ~10 to the overall discrimination.

The error frequency of *Escherichia coli* translation *in vivo* on internal codons was estimated to be in the range 6×10^{-4}–5×10^{-3}, on average 3×10^{-3} (Kurland and Ehrenberg, 1987). The error frequency measured *in vitro* at 10 mM Mg^{2+} is 10 times higher; there is essentially no initial selection under these conditions, and the observed fidelity is due to proofreading only. Lowering the Mg^{2+} concentration to 5 mM improves the selectivity of aa-tRNA binding and overall translation to $1–3\times10^{-3}$, which is close to values found *in vivo*. The increase in selectivity results mainly from improved initial selection which, at the lower Mg^{2+} concentration, contributes a factor of 10 to the overall fidelity, while the contribution of proofreading is increased only ~2-fold, to a factor of ~100. These values are probably representative of the contributions of initial selection and proofreading to the overall fidelity *in vivo*.

For comparison, the selectivity in a non-cognate situation was also calculated, using previously published rate constants (Rodnina *et al*., 1996). For the binding of EF-Tu·GTP·Phe-tRNA^{Phe} to poly(A)-programed ribosomes, the resulting k_{cat}/K_M value is 5×10^{-3}/s /0.42 μM = 0.012/μM/s (10 mM Mg^{2+}). Thus, the error frequency of initial selection of non-cognate ternary complexes is 1.4×10^{-4}, predicting an error of ~3×10^{-3} in initial selection assuming a 20-fold excess of non-cognate over cognate ternary complexes. Thus, discrimination against non-cognate ternary complexes can be achieved in a single round of selection with essentially no cost with respect to GTP hydrolysis.

Discussion

Four rate constants are affected when an A–U base pair in the codon–anticodon duplex is replaced with a G–U mismatch in the first position of the codon, as in the present comparison of Phe and Leu. The rate constants of the two dissociation steps, k_{-2} and k_7 (Figure 1), increase by factors of 100 and at least 20, respectively. These differences reflect the different stabilities of cognate and near-cognate codon–anticodon complexes prior to GTPase activation and A-site accommodation, respectively, which contribute to the discrimination by rejection in initial

selection and proofreading. However, two forward reactions are affected. The GTPase rate constant, k_3, is lowered 10-fold in the near-cognate compared with the cognate complex, and the rate constant of aa-tRNA accommodation, k_5, is decreased ~60 times. In both cases, rearrangements are affected that limit the rates of the following irreversible chemical steps (GTP hydrolysis and peptide bond formation) and are likely to lead to the respective transition state complexes. This suggests the existence of yet another selection mechanism, in addition to discrimination by rejection, i.e. discrimination by induced fit, which contributes to both initial selection and proofreading. The quantitative analysis shows, as discussed below, that only the combined contribution of both selection mechanisms accounts for the fidelity levels determined both *in vitro* and *in vivo*.

The differences in the stabilities of cognate and near-cognate aa-tRNA prior to or following GTP hydrolysis have been shown previously. Thus, Thompson and colleagues reported 10^3- to 10^4-fold different stabilities of cognate and near-cognate codon–anticodon complexes on the ribosome, and an at least 75 times higher rejection rate for a near-cognate aa-tRNA in the proofreading step (5 mM Mg^{2+}, 4°C; Thompson and Dix, 1982). Our data are in qualitative agreement with these results, and the differences in the absolute values of the rate constants can be readily explained by different ionic and temperature conditions.

The rate constants of the chemical steps, GTP hydrolysis and peptide bond formation, have been reported previously to be similar for cognate, near-cognate and non-cognate ternary complexes, which constituted the basis for the internal kinetic standard model (Thompson, 1988). However, the rates of GTP hydrolysis were not determined with precision (20/s and >4/s for the cognate and near-cognate ternary complex, respectively; Eccleston *et al*., 1985), and the rate constants of codon recognition and GTP hydrolysis were not distinguished, as there was no independent information for the former step. Rate constants of peptide bond formation were calculated to be between 0.3 and 1.1/s for cognate Phe-$tRNA^{Phe}$ and ~0.3 ± 0.15/s for near-cognate Leu-$tRNA_2^{Leu}$ (Thompson and Dix, 1982; Eccleston *et al*., 1985). Thus, the differences in the rate constants of GTP hydrolysis and peptide bond formation in the cognate and near-cognate cases which we observe were overlooked previously. Therefore, an essential premise of the internal kinetic standard model for translational accuracy ('internal clock' model) (Thompson, 1988) is not valid.

The finding that both rejection and induced-fit discrimination are important for aa-tRNA selection allows us to explain a number of earlier observations which were difficult to understand solely on the basis of different rejection rates of cognate and near-cognate aa-tRNA. It was shown that the rate constant of GTP hydrolysis during A-site binding is substantially smaller in SmD and SmP mutants in relation to wild-type ribosomes (Bilgin *et al*., 1992). These S12 mutants, in the absence of streptomycin, are error restrictive (Gorini, 1971), and it was argued that the increase in fidelity is due to improved initial selection (Bilgin *et al*., 1992) rather than to increased proofreading (Ruusala *et al*., 1984). The present model is in line with these observations, as it predicts that a decrease of the GTPase rate will improve the efficiency of initial selection.

Also not compatible with previous selection models was the observation that tRNA mutants lacking the standard D arm–T arm tertiary interactions are error-prone (Yarus and Smith, 1995). It has been postulated that distortions of the tRNA molecule ('waggle') contribute to differential stability of cognate and near-cognate aa-tRNA on the ribosome, and thus to the fidelity in selecting ternary complexes. Two lines of evidence are in line with tRNA distortions taking place upon codon recognition. First, based on fluorescence quenching measurements, the tRNA was found to assume an open conformation of the D loop after codon recognition (Rodnina *et al*., 1994). Secondly, electron cryomicroscopy of the EF-Tu·GTP·aa-tRNA complex on the ribosome shows a significant displacement of the anticodon arm of the tRNA compared with the crystal structure of the free ternary complex (Stark *et al*., 1997). It seems that the distortion of the tRNA molecule depends upon correct base pairing and may contribute to the activation of GTP hydrolysis in EF-Tu. The increased flexibility of mutant tRNAs lacking some tertiary structure interactions could allow more efficient activation of the GTPase because the tRNA is more easily distorted, in cognate as well as in near-cognate cases, and thus lead to a lower fidelity of aa-tRNA selection.

The finding that the rate constants of both rejection and accommodation differ for cognate and near-cognate aa-tRNA may also explain enhanced translational misreading caused by mutations in the peptidyltranferase region of 23S rRNA (Gregory *et al*., 1994; O'Connor and Dahlberg, 1995). Upon accommodation, the 3′ end of aa-tRNA is bound to the peptidyltransferase region, presumably by direct base pairing with 23S rRNA (Samaha *et al*., 1995). rRNA mutations that impair this interaction directly, or indirectly by changing the conformation of rRNA, may lead to a decreased accommodation rate, particularly for cognate aa-tRNA, thereby reducing both growth rate and translational accuracy.

The present model of an induced-fit mechanism of aa-tRNA discrimination places the ribosome beside DNA polymerases and RNA polymerase for which analogous models have been put forward. Extensive results obtained for DNA polymerases suggest that there is additional discrimination, apart from exonuclease proofreading, at the level of nucleotide incorporation, in that correct nucleotides are incorporated much faster than incorrect ones (Johnson, 1993; Rittinger *et al*., 1995; Spence *et al*., 1995). The kinetic contribution to selection in these models is due to the acceleration of the forward reactions of the cognate substrate as compared with the non-cognate ones. Direct evidence suggesting that structural differences between correct and incorrect base pairs influence the catalytic center of the DNA polymerase by induced fit is provided by crystal structures (Doublié *et al*., 1998; Kiefer *et al*., 1998; Li *et al*., 1998). A similar mechanism appears to operate in *E.coli* RNA polymerase (Erie *et al*., 1993).

In these systems, induced fit can enhance fidelity because rearrangements of the enzyme–substrate complexes, and not the chemical steps, are rate-limiting and are accelerated for the correct substrates (Herschlag, 1988; Post *et al*., 1995). Otherwise, as has been pointed

out (Fersht, 1985), induced fit would not increase fidelity, since the structure of the transition state is the same for every substrate. In the case of the ribosome, the respective rate-limiting rearrangements that are affected by structural details of codon recognition are GTPase activation and A-site accommodation.

How the ribosome senses structural differences between cognate and near-cognate codon–anticodon duplexes and how these differences may affect the GTPase activation and accommodation steps is not known. One attractive possibility is that the formation of the codon–anticodon duplex induces a conformational change in the decoding center, presumably in the 16S rRNA, and that the rate of this change depends upon structural details, such as potential hydrogen bonds, which are provided by the cognate, and less so by the near-cognate, codon–anticodon duplex (Powers and Noller, 1994; Fourmy *et al*., 1996, 1998). The induced conformational change may constitute the signal that is transmitted to the G domain of EF-Tu to trigger the GTPase. The transmission may be accomplished either by a series of subsequent conformational changes of the ribosome traveling across the subunit interface or, as mentioned above, by a movement (or distortion) of the tRNA molecule that is induced by the conformational change of the decoding center.

The model also explains how a cognate, more efficiently than a near-cognate, codon–anticodon duplex may promote the accommodation of the aa-tRNA in the A-site. In order to reach the peptidyltransferase center, the acceptor arm has to move into the 50S A-site after it has been released from EF-Tu. According to the structural reconstruction of the codon recognition complex by electron cryomicroscopy (Stark *et al*., 1997), the movement involves a rotation of the whole tRNA molecule pivoting around the anticodon. It is conceivable that conformational changes in the decoding center are instrumental in promoting the rotational movement of the tRNA. In this model, the rate of accommodation is determined by the rate of the conformational change in the decoding center, and the latter, in turn, is promoted by structural determinants provided by the cognate, and less so by the near-cognate, codon–anticodon duplex.

Materials and methods

Biochemical assays

Materials were as described previously (Rodnina *et al*., 1994, 1995, 1996; Vorstenbosch *et al*., 1996; Pape *et al*., 1998). Ternary complexes, EF-Tu·GTP·aa-tRNA, were purified by gel filtration on Superdex 75 in buffer A (50 mM Tris–HCl, pH 7.5, 50 mM NH_4Cl, 10 mM $MgCl_2$, 1 mM dithiothreitol). To fill the P-site, ribosomes were incubated in buffer A for 15 min at 37°C with a 1.3-fold excess of AcPhe-tRNA^{Phe} and 1 mg/ml of poly(U). For the determination of dipeptide formation, purified EF-Tu·GTP·[^{3}H]Leu-tRNA$_2^{Leu}$ complex (20 000 d.p.m./pmol) and, where necessary, EF-Tu·GTP·[^{14}C]Phe-tRNA^{Phe} (1060 d.p.m./pmol) were added. GTP hydrolysis was measured with ternary complexes containing [γ-^{32}P]GTP (1000 d.p.m./pmol).

Kinetic experiments

Stopped-flow and quench-flow measurements were carried out and the data evaluated as described previously (Rodnina *et al*., 1994, 1995, 1996; Vorstenbosch *et al*., 1996; Pape *et al*., 1998). The experiments were performed at 20°C by rapidly mixing equal volumes (stopped flow, 60 µl; quench flow, 26 µl) each of the purified ternary complex (0.1 µM after mixing) and the ribosome complex (0.3–2.0 µM). Apparent rate constants were determined by exponential fitting, using one or two exponential terms (characterized by variable time constants, k_{app}, and respective amplitudes) and another variable for the final signal. Elemental rate constants were calculated by global fitting of combined sets of time courses measured at several different ribosome concentrations by proflavin and mant-dGTP fluorescence, GTP hydrolysis and dipeptide formation. Fitting was performed by numerical integration using Scientist for Windows software (MicroMath Scientific Software) (Pape *et al*., 1998). For this purpose, the kinetic scheme of Figure 1 was modified as follows:

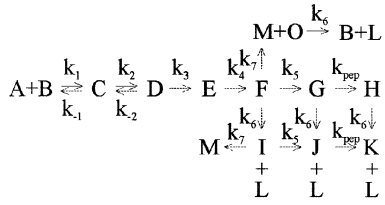

EF-Tu and ribosome complexes are designated as A and B, respectively. The formation of the initial binding complex C is followed by codon recognition (D). The following steps of GTPase activation and GTP hydrolysis are not distinguished kinetically, and were therefore grouped, leading to formation of a transient complex E. The conformational change of EF-Tu from the GTP to GDP form results in an intermediate F. aa-tRNA is accommodated in the A site (G) and can take part in peptide bond formation (H). The timing of EF-Tu·GDP dissociation from the ribosome is not known. Therefore, we assumed that it can dissociate at any time point after the formation of the GDP form of EF-Tu, i.e. from intermediates F, G and H, resulting in complexes I, J and K, as well as free EF-Tu·GDP (L). With respect to the state of aa-tRNA on the ribosome, states F and I, G and J, as well as H and K are equivalent and represent the complexes after release from EF-Tu (F and I), accommodation (G and J) and peptide bond formation (H and K). Alternatively, aa-tRNA can be rejected from the ribosome (M), before or after the release of EF-Tu·GDP. In the former case, the ribosome·EF-Tu·GDP complex (O) dissociates to give the ribosome (B) and EF-Tu·GDP (L).

The overall fluorescence is determined by the concentration of the fluorescent species, and their respective relative fluorescence. For the calculations, the fluorescence of proflavin in the free ternary complex (P_A) was set to 10 for 1 µM concentration, so that the fluorescence of 0.1 µM ternary complex (standard concentration) is 1. The formation of the initial binding complex C leads to an increase of fluorescence to P_C = 10.6 for Leu-tRNA$_2^{Leu}$(Prf16/17/20) (Rodnina *et al*., 1996). The fluorescence changes further in the codon–anticodon complex D to P_D = 12 for Leu-tRNA$_2^{Leu}$(Prf16/17/20). GTP hydrolysis and the conformational rearrangement of EF-Tu do not change proflavin fluorescence; therefore, the same relative fluorescence P_D can be used for the intermediates E, F and I. Only 1.5% of Leu-tRNA$_2^{Leu}$ is accommodated in the A site, therefore the fluorescence of the intermediates G, H, J and K is poorly defined. Most of aa-tRNA is rejected; the fluorescence of free aa-tRNA P_M = 11. The overall proflavin fluorescence is $F_{Prf} = P_A{\cdot}A + P_C{\cdot}C + P_D{\cdot}(D + E + F + I) + P_G{\cdot}(G + H + J + K) + P_M{\cdot}M$.

The fluorescence of the mant group is set to 10 for the free ternary complex (M_A at 1 µM). It increases upon GTPase activation (intermediate E, relative fluorescence M_E = 13.3), and decreases to about the starting level upon dissociation of EF-Tu·GDP from the ribosome (complex L, relative fluorescence M_L) (Rodnina *et al*., 1995). The overall mant fluorescence $F_{Mant} = M_A{\cdot}(A + C + D) + M_E{\cdot}(E + F + G + H) + M_L{\cdot}L$.

For calculations, the values of k_{-1}, P_A and P_C (determined previously; Rodnina *et al*., 1996), as well as k_{-2} (determined independently, this study), were fixed. The fitting yields a unique solution for the rate constants k_1–k_7, as well as for the remaining fluorescence factors. The error limits of the kinetic parameters are given in Table I. For values that were measured directly, the given standard deviation is calculated from the results of several experiments. For values calculated by global fitting, the standard deviation for a given parameter was determined for the case when all other parameters, except the fixed ones, are allowed to change. That is, if a given parameter is set to a value that is outside the range of standard deviation, there is no fit satisfying all data sets.

Determination of selectivity from elemental rate constants

The ratio of the A-site binding rates of correct (v_c) and incorrect (v_i) aa-tRNA depends on the selectivity (S) and the ratio of concentrations of correct (c_c) and incorrect (c_i) ternary complexes (Fersht, 1985):

$$\frac{v_c}{v_i} = S \cdot \frac{c_c}{c_i} \quad (1)$$

The overall selectivity of aa-tRNA binding S is determined as a product of initial selection f and proofreading F:

$$S = f \times F \quad (2)$$

The efficiency of initial selection is defined as the ratio of correct and incorrect k_{cat}/K_M:

$$f = \frac{k^c_{cat}/K^c_M}{k^i_{cat}/K^i_M} \quad (3)$$

The value of k_{cat}/K_M is determined by the rate constants of the binding steps, k_1, k_{-1}, k_2 and k_{-2}, and the GTPase rate constant, k_3 (Figure 1). Since the values of k_2 and k_3 are comparable, the expression for k_{cat}/K_M was derived using the steady-state approximation which yields:

$$k_{cat}/K_M = \frac{K_1 \cdot k_2 \cdot k_3}{(k_{-1} + k_2) \cdot (k_{-2} + k_3) - k_{-2} \cdot k_2} \quad (4)$$

The values of k_{cat}/K_M for cognate and near-cognate aa-tRNA were calculated with the respective rate constants for Phe and Leu, and then used to determine the efficiency of initial selection, f (Equation 3). The equations defining the error frequency, P_e, were taken from Ehrenberg *et al*. (1990).

Acknowledgements

We thank Roger Goody for generous gifts of mant nucleotides, Yuri Semenkov and Vladimir Katunin for purified tRNA, Petra Striebeck for expert technical assistance, and Dmitri Rodnin for computer programing. The work was supported by the Deutsche Forschungsgemeinschaft (Wi 626/11-1), the Alfried Krupp von Bohlen und Halbach-Stiftung and the Fonds der Chemischen Industrie. T.P. acknowledges a doctoral fellowship of the Werner Richard–Dr Carl Dörken-Stiftung.

References

Abel,K., Yoder,M.D., Hilgenfeld,R. and Jurnak,F. (1996) An α to β conformational switch in EF-Tu. *Structure*, **4**, 1153–1159.

Bilgin,N., Claesens,F., Pahverk,H. and Ehrenberg,M. (1992) Kinetic properties of *Escherichia coli* ribosomes with altered forms of S12. *J. Mol. Biol.*, **224**, 1011–1027.

Dell,V.A., Miller,D.L. and Johnson,A.E. (1990) Effects of nucleotide- and aurodox-induced changes in elongation factor Tu conformation upon its interactions with aminoacyl tranfer RNA. A fluorescence study. *Biochemistry*, **29**, 1757–1763.

Doublié,S., Tabor,S., Long,A.M., Richardson,C.C. and Ellenberger,T. (1998) Crystal structure of bacteriophage T7 DNA replication complex at 2.2 Å. *Nature*, **391**, 251–259.

Eccleston,J.F., Dix,D. and Thompson,R.C. (1985) The rate of cleavage of GTP on the binding of Phe-tRNA·elongation factor Tu·GTP to poly(U)-programmed ribosomes of *Escherichia coli*. *J. Biol. Chem.*, **260**, 16237–16241.

Ehrenberg,M. and Blomberg,C. (1980) Thermodynamic constraints on kinetic proofreading in biosynthetic pathways. *Biophys. J.*, **31**, 333–358.

Ehrenberg,M., Bilgin,N. and Kurland,C.G. (1990) Design and use of a fast and accurate *in vitro* translation system. In Spedding,G. (ed.), *Ribosomes and Protein Biosynthesis—A Practical Approach.* IRL Press, Oxford, UK, pp. 101–129.

Erie,D.A., Hajiseyedjavadi,O., Young,M.C. and von Hippel,P.H. (1993) Multiple RNA polymerase conformations and GreA: control of the fidelity of transcription. *Science*, **262**, 867–873.

Fersht,A. (1985) *Enzyme Structure and Mechanism*. W.H.Freeman and Co., New York, NY.

Fourmy,D., Recht,M.I., Blanchard,S.C. and Puglisi,J.D. (1996) Structure of the A site of *Escherichia coli* 16S ribosomal RNA complexed with an aminoglycoside antibiotic. *Science*, **274**, 1367–1371.

Fourmy,D., Yoshizawa,S. and Puglisi,J.D. (1998) Paromomycin binding induces a local conformational change in the A-site of 16S rRNA. *J. Mol. Biol.*, **277**, 333–345.

Gorini,L. (1971) Ribosomal discrimination of tRNAs. *Nature*, **234**, 261–264.

Gregory,S.T., Lieberman,K.R. and Dahlberg,A.E. (1994) Mutations in the peptidyl transferase region of *E.coli* 23S rRNA affecting translational accuracy. *Nucleic Acids Res.*, **22**, 279–284.

Herschlag,D. (1988) The role of induced fit and conformational changes of enzymes in specificity and catalysis. *Bioorg. Chem.*, **16**, 62–96.

Hopfield,J.J. (1974) Kinetic proofreading: a new mechanism for reducing errors in biosynthetic processes requiring high specificity. *Proc. Natl Acad. Sci. USA*, **71**, 4135–4139.

Johnson,K.A. (1993) Conformational coupling in DNA polymerase fidelity. *Annu. Rev. Biochem.*, **62**, 685–713.

Kaziro,Y. (1978) The role of guanosine-5′-triphosphate in polypeptide chain elongation. *Biochim. Biophys. Acta*, **505**, 95–127.

Kiefer,J.R., Mao,C., Braman,J.C. and Beese,L.S. (1998) Visualizing DNA replication in a catalytically active *Bacillus* DNA polymerase crystal. *Nature*, **391**, 304–307.

Kurland,C.G. and Ehrenberg,M. (1987) Growth-optimizing accuracy of gene expression. *Annu. Rev. Biophys. Biophys. Chem.*, **16**, 291–318.

Li,Y., Korolev,S. and Waksman,G. (1998) Crystal structures of open and closed forms of binary and ternary complexes of the large fragment of *Thermus aquaticus* DNA polymerase I: structural basis for nucleotide incorporation. *EMBO J.*, **17**, 7514–7525.

Ninio,J. (1975) Kinetic amplification of enzyme discrimination. *Biochimie*, **57**, 587–595.

O'Connor,M. and Dahlberg,A.E. (1995) The involvement of two distinct regions of 23S ribosomal RNA in tRNA selection. *J. Mol. Biol.*, **254**, 838–847.

Pape,T., Wintermeyer,W. and Rodnina,M.V. (1998) Complete kinetic mechanism of elongation factor Tu-dependent binding of aminoacyl-tRNA to the A site of the *E.coli* ribosome. *EMBO J.*, **17**, 7490–7497.

Polekhina,G., Thirup,S., Kjeldgaard,M., Nissen,P., Lippmann,C. and Nyborg,J. (1996) Helix unwinding in the effector region of elongation factor EF-Tu–GDP. *Structure*, **4**, 1141–1151.

Post,C.B. and Ray,W.J.,Jr (1995) Reexamination of induced fit as determinant of substrate specificity in enzymatic reactions. *Biochemistry*, **34**, 15881–15890.

Powers,T. and Noller,H. (1994) The 530 loop of 16S rRNA: a signal to EF-Tu? *Trends Genet.*, **10**, 27–31.

Rittinger,K., Divita,G. and Goody,R.S. (1995) Human immunodeficiency virus reverse transcriptase substrate-induced conformational changes and the mechanism of inhibition by nonnucleoside inhibitors. *Proc. Natl Acad. Sci. USA*, **92**, 8046–8049.

Rodnina,M.V., Fricke,R. and Wintermeyer,W. (1994) Transient conformational states of aminoacyl-tRNA during ribosome binding catalyzed by elongation factor Tu. *Biochemistry*, **33**, 12267–12275.

Rodnina,M.V., Fricke,R., Kuhn,L. and Wintermeyer,W. (1995) Codon-dependent conformational change of elongation factor Tu preceding GTP hydrolysis on the ribosome. *EMBO J.*, **14**, 2613–2619.

Rodnina,M.V., Pape,T., Fricke,R., Kuhn,L. and Wintermeyer,W. (1996) Initial binding of the elongation factor Tu·GTP·aminoacyl-tRNA complex preceding codon recognition on the ribosome. *J. Biol. Chem.*, **271**, 646–652.

Ruusala,T., Andersson,D., Ehrenberg,M. and Kurland,C.G. (1984) Hyper-accurate ribosomes inhibit growth. *EMBO J.*, **3**, 2575–2580.

Samaha,R.R., Green,R. and Noller,H.P. (1995) A base pair between tRNA and 23S rRNA in the peptidyl transferase centre of the ribosome. *Nature*, **377**, 309–314.

Spence,R.A., Kati,W.M., Anderson,K.S. and Johnson,K.A. (1995) Mechanism of inhibition of HIV-1 reverse transcriptase by nonnucleoside inhibitors. *Science*, **267**, 988–992.

Stark,H., Rodnina,M.V., Rinke-Appel,J., Brimacombe,R., Wintermeyer,W. and van Heel,M. (1997) Visualization of elongation factor Tu on the *Escherichia coli* ribosome. *Nature*, **389**, 403–406.

Thompson,R.C. (1988) EF-Tu provides an internal kinetic standard for translational accuracy. *Trends Biochem Sci.*, **13**, 91–93.

Thompson,R.C. and Dix,D.B. (1982) Accuracy of protein biosynthesis. A kinetic study of the reaction of poly(U)-programmed ribosomes with a leucyl-$tRNA_2$–elongation factor Tu–GTP complex. *J. Biol. Chem.*, **257**, 6677–6682.

Vorstenbosch,E., Pape,T., Rodnina,M.V., Kraal,B. and Wintermeyer,W. (1996) The G222D mutation in elongation factor Tu inhibits the codon-induced conformational changes leading to GTPase activation on the ribosome. *EMBO J.*, **15**, 6766–6774.

Yarus,M. and Smith,D. (1995) tRNA on the ribosome: a waggle theory. In Söll,D. and RajBhandary,U. (eds), *tRNA: Structure, Biosynthesis, and Function*. American Society for Microbiology, Washington, DC, pp. 443–468.

Received February 10, 1999; revised and accepted May 3, 1999